Solid-State Electronics Vol. 25, No. 3, pp. 185–195, 1982
Printed in Great Britain

0038-1101/82/030185-11$03.00/0
Pergamon Press Ltd.

CHARACTERISTICS OF AuGeNi OHMIC CONTACTS TO GaAs

M. HEIBLUM, M. I. NATHAN and C. A. CHANG
IBM Thomas J. Watson Research Center, P.O. Box 218, Yorktown Heights, NY 10598, U.S.A.

(*Received* 5 *May* 1981; *in revised form* 20 *July* 1981)

Abstract—We have studied AuGeNi ohmic contacts to n-type MBE grown GaAs epitaxial-layer with doping in the (10^{16}–10^{19}) cm^{-3} range, and found several new effects: (a) Contact resistivity exhibit a weak dependence on carrier concentration (much weaker than $1/N_D$ dependence); (b) We find evidence for a high resistivity layer under the contact at least several thousands angstroms deep, which dominate the contact resistance in most cases; (c) We find a peripheral zone around the contact, about 1 μm wide which differs chemically from the GaAs epi-layer; (d) SIMS analysis reveals a deep diffusion into the GaAs of Ni and Ge; (e) Correlation between density of GeNi clusters in the contact and the contact resistivity are found; (f) Temperature measurements justify that tunneling is responsible for the ohmic contact. We discuss also the validity of the transmission line method and the commonly accepted model of the contact.

1. INTRODUCTION

The need for a reliable ohmic contact to n-type GaAs emerged in the late sixties after the discovery of the Gunn effect. Consequently, the AuGe eutectic mixture was used[1]. Since then, it has provided the lowest resistance, most reliable, convenient, and widely used ohmic contact.

The AuGe ohmic contact is usually formed by evaporating a eutectic mixture of AuGe (88–12%, respectively) followed by a thin layer of Ni. It is then alloyed in H_2 environment (or forming gas) for a minute or so at 450°C. It is believed that Ge dopes the underlying GaAs heavily so that tunneling may occur through the formed Au–GaAs Schottky barrier. Ni was added originally to maintain a smooth surface morphology during the alloying process[1], but it was recognized later that it improves the contact's adherence to the surface and its electrical properties.

A large number of papers had been published on the subject. Most investigated the metallurgical structure of the contact, and a few electrical properties. The only evidence that Ge forms an n^+-layer near the contact was provided by Holonyak *et al.*[2, 3], in fabricating a tunnel junction by alloying of AuGe contact onto a p^+-type GaAs. The n^+-doping was estimated at $(3\text{–}5)\times 10^{18}\ cm^{-3}$ [3, 4]. The effective barrier height after alloying was measured by Paria *et al.* to be 0.3 eV[5]. We have also carried temperature measurements and confirm the proposed tunneling model.

In the initial utilization of the AuGe ohmic contact, Gunn reported the existence of a high resistivity layer under one of two symmetric contacts[6]. Hasty *et al.* reported of a similar observation on a similar contact (AgGeIn), where a layer doped to $5\times 10^{14}\ cm^{-3}$ in a $2\times 10^{15}\ cm^{-3}$ doped material was suggested to occur[7]. Similar suggestions can be found in Refs. [8–10], and opposing results in [11, 12]. In Ref. [11] the authors observe an unexpected long n-type doping tail of $(1\text{–}2)\times 10^{16}\ cm^{-3}$ under the contact, and in [12], the author reports on AuIn contacts. Finding the contact resistivity relies on the utilization of the "Transmission Line Method" (TLM)[17–23], where the determination of the resistance under the contact is very important. The possibility of high resistivity layer is always ignored. We have measured directly the resistivity as a function of depth under the contact, and observed a high resistance layer which can be a dominating factor in the contact resistance.

The redistribution, diffusion and recrystallization of Au, Ge, Ni, Ga and As after alloying is extremely complicated and not well understood. The surface does not melt and recrystallize homogenously and uniformly. Many attempts to understand the underlying layer have been reported utilizing Rutherford back scattering, Auger microscopy, stress measurements, electron microscopy, and electrical measurements. Harris *et al.* reported a decomposed layer, 0.1 μm thick, with high conductivity under the contact, from C–V measurements[11]. Inada *et al.*, utilizing the sputtering-Auger technique, reported a decomposed layer of 0.11 μm deep under the contact[13], which they assumed to be conductive. Similarly, Ogawa reported on a decomposed GaAs layer which is 0.19 μm thick, independent of the alloying time[14]. Recently, Miller reported a penetration depth of the contact between 0.45 and 1.4 μm[15]. As far as we know, the electrical properties of the decomposed layer have not been measured but it has been assumed by most researches that it has the same conductivity as the uncontacted material or a metallic behavior[11–13]. As we mentioned above we have strong evidence that there is a layer under the contact whose resistance is higher than that of the uncontacted layer, and this layer extends deep into the material.

It was realized early that the individual diffusion of Au, Ge and Ni is drastically changed when they coexist on the GaAs wafer. For example, Au by itself will not completely penetrate into the GaAs at 500°C until 12 min, while AuGe is consumed after 1 min of heating to only 450°C[14, 24]. Also, Ge by itself does not diffuse deep in a heating process, but Ge in the presence of Ni

diffuses to a depth of a few thousand angstroms into the GaAs (together with the Ni)[8, 14, 25–29].

Morphology of the surface after alloying is never uniform. Viewing the top with a light or a scanning electron microscope reveals dark regions in cluster form of 0.5 μm to few microns in size, which have been identified as Ge and Ni rich[10, 14, 25, 27]. A correlation between particles size and the contact resistivity had been found[26, 27]. We have observed a correlation too, but with opposite trends.

Scanning along the depth dimension under the alloyed contact reveals a heterogenous structure. The sequence of evaporation does not seem to matter to the final arrangement of the constituents. It seems that mostly Ga and to less extent As diffuse through the top metallurgy to the surface and Ge and Ni move deep into the GaAs[4, 31, 32]. Immediately under the contact a highly disordered region occurs. Gold precipitates, and hexagonal AuGa rich regions with high density of dislocation lines extending through to more than 3000 Å deep appear[33]. We have looked at the underlayer contact with Secondary Ion Mass Spectrometry (SIMS) and observed deep penetration of Ge and Ni into the GaAs.

It is believed now that the Ni enhances the indiffusion of Ge (also by increasing the solubility of GaAs in AuGeNi melt), and Au enhances the outdiffusion of Ga, so that most of the Ge sits on substitutional Ga sites and creates the desirable n^+-layer (normally Ge is an amphoteric dopant in GaAs)[24, 35, 36]. It was also noted that an excess of Au[35–37], or Ni[14, 34, 38] degrades the contact resistivity. Excess Au, most probably, leads to excess Ga outdiffusion which leaves excess As and not enough Ge to replace the Ga. Also, Au and Ni act as acceptors and may compensate the underlying n^+-layer (not to mention degradation due to damage). It is advisable to use thin contact layers to form ohmic contacts and to enhance the conductivity of the contact by post-alloy deposition, or a pre-alloy deposition with some barrier layer[34, 35] which will prevent indiffusion of top metallurgy into the contact region.

Most reliable measurements of contact resistivity are done by utilizing the TLM on epi-layers grown on insulating substrates[17–23], because the intrinsic resistance of the contacted layer is accurately subtracted. A much less accurate method, proposed by Cox and Starck[39], is the "Vertical Transport Method" (VTM). It is generally believed that the contact resistivity decreases when the carrier concentration in the epi-layer increases (usually with a $1/N_D$ dependence). This has been observed by both TLM and VTM[13, 40–45]. However, since the Ge always dopes the epi-layer to the same n^+-concentration, it is not obvious that the contact resistivity should drop with increasing the epi-layer carrier concentration. Popovič proposed an explanation assuming that the n^+-region is so thin that ballistic transport of electrons is possible through it, so that the boundary at the n^+ (due to Ge doping)—n (epi) layers affects the contact resistivity[46]. We have measured the contact resistivity on relatively thick epi-layers and gotten a weak dependence of contact resistivity (ρ_c) on carrier concentration in the range $(10^{16}\text{–}10^{19})\ \text{cm}^{-3}$. We suggest that this measured effect results from the high resistivity layer under the contact and other geometrical effects which solely depend on the measuring technique.

In this paper we report results of an extensive study of AuGeNi ohmic contacts on n-type GaAs. We have carried out SIMS and microprobe studies to reveal the properties of top and underlying layers. In addition, we have utilized the TLM and a variation of it to characterize electrically the contacted material for carrier concentrations in the range $(10^{16}\text{–}10^{19})\ \text{cm}^{-3}$. We have also conducted temperature measurements to identify the mechanism of current conduction. We point out the limitations of the TLM, and suggest that the intrinsic contact resistivity is probably lower than the routinely measured one.

2. CONTACT PREPARATION

Contacts were made on MBE grown epitaxial layers. The layers' thicknesses covered the range of (0.1–2.5) μm and doping levels of $(10^{16}\text{–}10^{19})\ \text{cm}^{-3}$. Before growth, semi-insulating GaAs substrates with (100) orientation were polished and chemically cleaned. In situ sputter-etching and thermal annealing were performed before an undoped buffer layer (mid $10^{14}\ \text{cm}^{-3}$ p-type) of about 2500 Å thickness was grown, followed by the epi-layer growth.

After withdrawal from the MBE system samples were processed for Hall and TLM measurements, SIMS and microprobe analyses. Where patterning was needed, a photoresist mask was prepared and the contact was evaporated on top, to be formed by a lift-off process later. Before contact evaporation onto the GaAs, the surface was cleaned by HF-vapor, rinsed thoroughly with deionized water, nitrogen dried, and immediately thereafter placed in a vacuum evaporator which was pumped down to 10^{-6} torr. Following the process devised by Vidimari[45], Ni was evaporated first ($\sim$ 50 Å), followed by Au ($\sim$ 450 Å), Ge ($\sim$ 200 Å), and SiO_2 ($\sim$ 1000 Å). All evaporations were done in a single pump down by an E-gun with four crucibles. After patterning, samples were alloyed in a forming-gas environment, on a carbon heater strip at 450°C for 30 sec, with rise and fall times of about 20 sec each. The SiO_2 was then etched-off with HF:H_2O (1:3). The resulting contacts look smooth with gold-like color, and speckeled with dark clusters, 0.5 μm to a few microns in size.

We will now describe in some detail each experimental procedure, and discuss the results.

3. CONTACT RESISTIVITY VS CARRIER CONCENTRATION

The measurement procedure exploits the "Transmission Line Method" (TLM)[17–23]. The method is described briefly, followed by the fabrication and measurement procedure and then the results.

(a) *Theory and limitations*

The name is derived from the close analogy to the analysis of a lossy transmission line. As shown in Fig. 1(a), the current I dissipates into the contact in a characteristic lenght l_t. The total resistance measured between the two metal contacts R_T, for $L \gg l_t$ is[21, 22].

$$R_T = (R_{sh}/Z)(l + 2l_t) \quad (1)$$

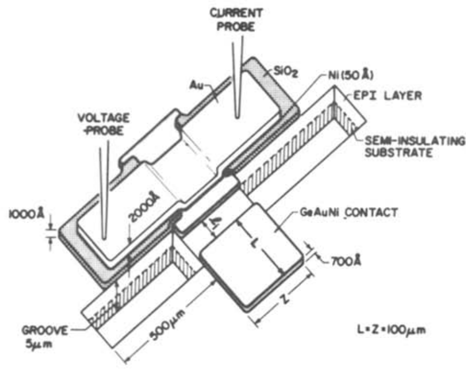

(a)

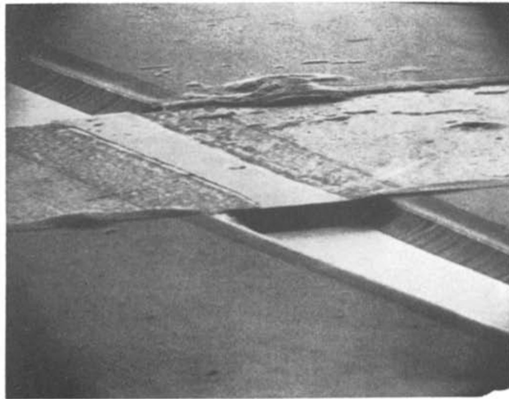

(b)

Fig. 2. A description f the fabricated structure for the TLM of measurements. (a) A drawing with major dimensions. The SiO_2 pads are 90 μm wide, and the overlay of Au is 75×500 μm. (b) An SEM picture of the actual structure (mag. ~ ×6000).

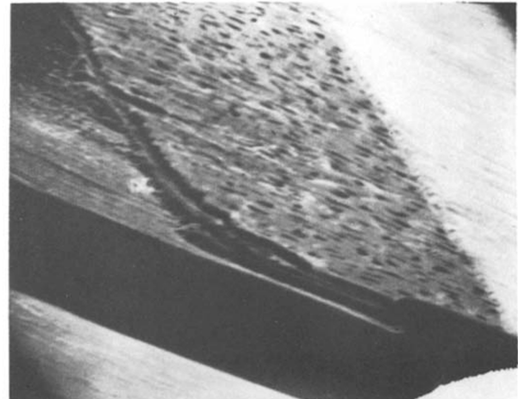

(a)

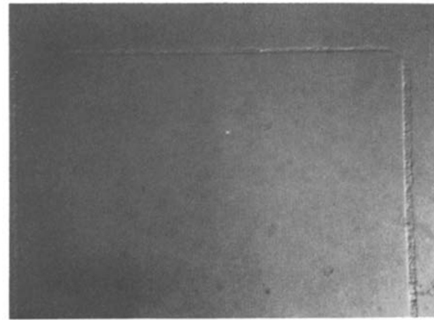

(b)

Fig. 7. Observed periphery-ridge after etching. (a) An SEM micrograph of the edge of the GeAuNi contact where etching of the GaAs was performed. An unetched step is clearly visible. (Mag. ~ 20,000) (b) An optical micrograph reveals a similar ridge around an evaporated and heated up Ni square. (The Ni is removed (Mag. ~ ×820)). Ridge width in both cases is about (1–2) μm.

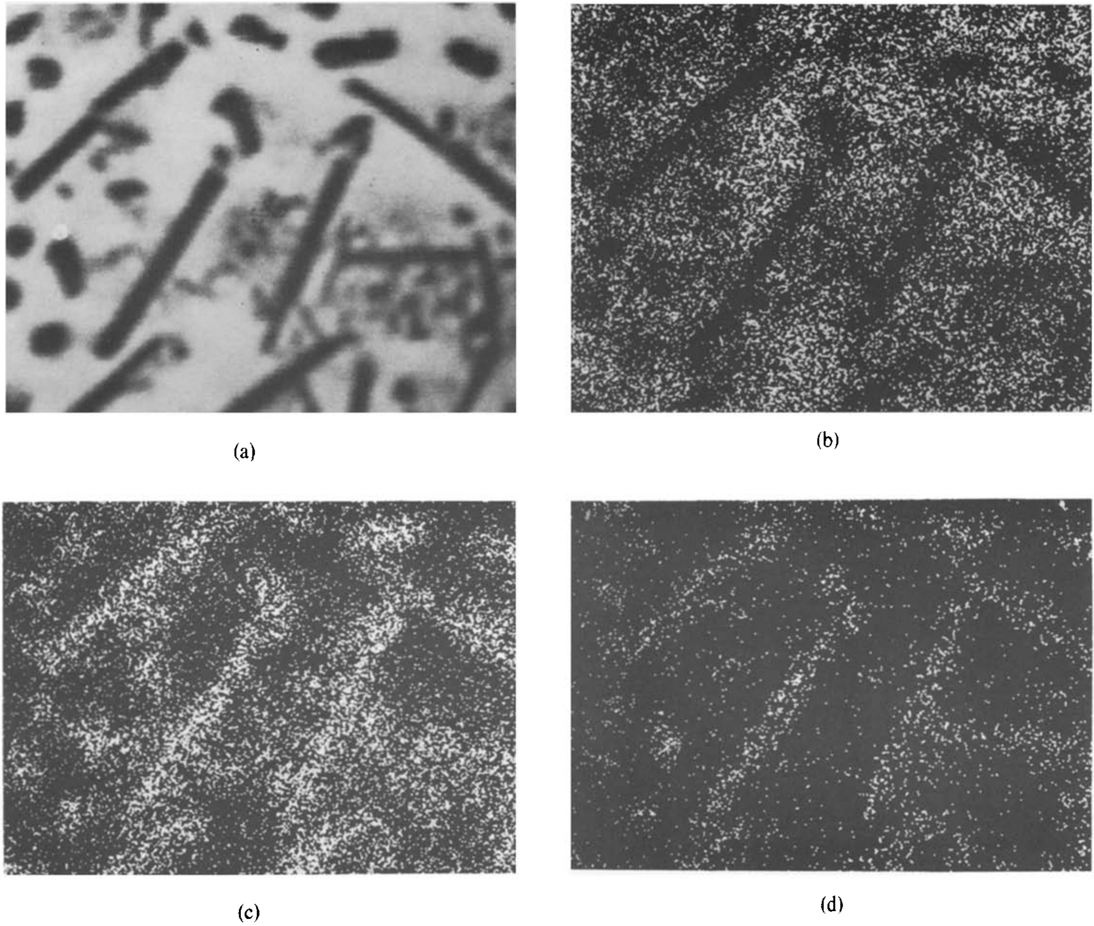

(a) (b) (c) (d)

Fig. 8. An SEM micrograph and microprobe results of top alloyed GeAuNi contact surface. The dark clusters visible are identified as Ge–Ni rich and Au deficient. (a) SEM; (b) Au ($M\alpha$ line); (c) Ge($L\alpha$ line); (d) Ni ($K\alpha$ line). Mag. ~ ×5000.

where $R_{sh} = \rho/t$ is the sheet resistance, and Z and L are defined in Fig. 2. The contact resistivity $\rho_c[\Omega\,cm^2]$ is given by

$$\rho_c = l_t^2 R_{sh}. \quad (2)$$

By measuring R_T as a function of l as shown in Fig. 1(b), one gets a straight line with slope R_{sh}/Z and an intercept with the ordinate at $-2l_t$. Note that in this model the vertical voltage drop under the contact is not included. Berger estimated this contribution which is important in cases when $\rho_c < 0.2\rho t$, arriving at[22]

$$\rho_c \cong \rho_c[\text{eqn (2)}] - 0.2\rho t, \quad (3)$$

which he has named the "Extended TLM" (or ETLM).

When the TLM is used, one should consider the following points: (1) An epi layer which is too thin might be depleted near the air-GaAs and substrate-epi layer interfaces (the depletion width are about 2000 Å and 100 Å for $10^{16}\,cm^{-3}$ and $10^{18}\,cm^{-3}$ doping, respectively), (2) A layer which is too thick allows only an approximate calculation of ρ_c, (3) The region underlying the contact can have specific resistivity which is entirely different from the uncontacted material, (4) The underlying layer is not homogeneous due to: n^+-Ge doped layer, Au and Ni diffused layers, non-uniform alloying, and dislocations caused by stresses, (5) Poor edge definition of contacts (due to non-uniform alloying and clusters) makes the determination of l inaccurate, (6) Resistivity of AuGeNi is higher after alloying[35, 47, and our measurements] and can contribute to a series resistance.

(b) *Experimental procedure*

We have checked the dependence of ρ_c on the carrier concentration of the epi layer. We have chosen to work with thick layers where the solution is approximate, but avoiding the more serious problems associated with thin layers (points (1), (3) and (4) above).

The test pattern is described in Fig. 1(b). Nine squares ($100 \times 100\,\mu m^2$ each) provided eight different gaps which were measured separately on each test pattern (nominal values: 3.5, 6, 8.5, 11, 13.5, 16, 18.5 and 21 μm). They were fabricated using the procedure described previously. To achieve best contact resistivity the GeAuNi layer was kept thin[35, 36], but in order to reduce the spreading resistance of the contact, a thicker layer of Au was evaporated after alloying ($\sim$2000 Å, on top of a 50 Å layer of Ni for adherence purposes), as shown in Fig. 2. We have measured resistances employing the four probe technique, and to avoid damage to the contact area the pads was extended outside the contact region (with SiO_2 buffer to avoid contact to the GaAs material, see Fig. 2(b)). Grooves, 5 μm deep, were etched to constrain current flow to the region $Z = 10\,\mu m$ wide. Fig. 2(a) gives in some detail a schematic representation of the structure of one of the contacts, and Fig. 2(b) is an SEM micrograpnh of an actual pattern. Fig. 3 provides a summary of results from measurements carried out on Ge doped epi-layers in the range, $(10^{16}\text{–}10^{18})\,cm^{-3}$, and Sn doped in the $10^{19}\,cm^{-3}$ range. Thicknesses are in the range of (1.5–4) μm on a 2500 Å undoped buffer layer (high $10^{14}\,cm^{-3}$, p-type), which is grown on top of Cr-doped semi-insulating GaAs substrates. Equation (3) and plots like in Fig. 4(b) were employed, with results from a few test patterns on each wafer and sometimes from more than one wafer. As seen in Fig. 3, the contact resistivity drops by $\sim$1.5 orders of magnitude from $1 \times 10^{-5}\,\Omega$ to $6 \times 10^{-7}\,\Omega\,cm^2$, while carrier concentration increases by 3 orders of magnitude, in contrast with[45]. The resistivity of the eip layer which is deduced from eqn (1) and checked by Van der Pauw method[48], is plotted too.

4. RESISTIVITY OF CONTACTED MATERIAL

We describe a variation of the TLM, which we call "Grooved TLM" (GTLM) and which enabled us to deduce the resistivity of the layer under the contact. This resistivity is of importance since it affects significantly the determination of ρ_c. However, measuring it is not straight forward. Attempts to remove the alloyed GeAuNi by chemical etching or ion milling resulted in an unavoidable penetration into the eip-material and with very poor surface quality.

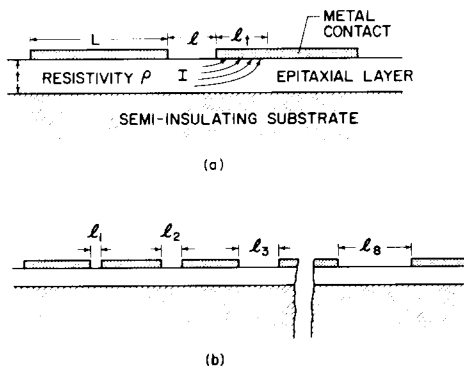

Fig. 1. Transmission Line Method (TLM) of measuring contact resistivity. (a) The current dissipates into the contact in a characteristic length l_t. (b) A schematic representation of a nine-pads, different l's TL experiment.

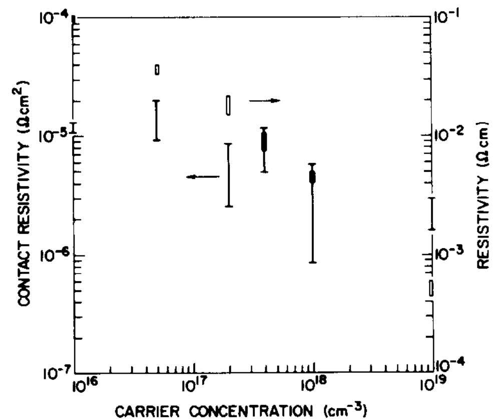

Fig. 3. Dependence of contact and epi-layer resistivities on carrier concentration. Note that over three orders of magnitude change in N_D, ρ_c changes by about one order of magnitude.

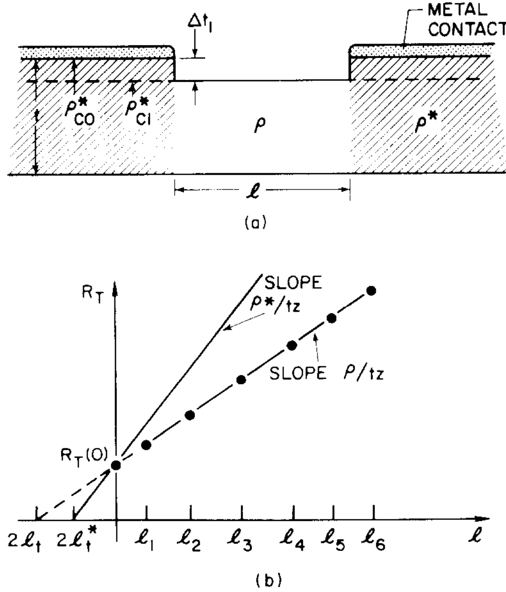

Fig. 4. Grooved TLM (GTLM) of measurements. (a) Etching grooves between the pads changes the measured ρ_{c0} to ρ_{c1}. Resistivity under the contact is ρ^* (rather than ρ). (b) As a result of ρ^* under the contact, the true l_t can be l_t^*, and ρ^* is found from the slope of the line.

Assume that the resistivity under the contact is some ρ^* and it uniformly extends through the epi-material (Fig. 4(b)). Before etching between the pads is performed, $\Delta t_1 = 0$ and a straight line describes R_T vs l. This line does not give the correct l_t (at the point $R_T(-2l_t) = 0$). The correct l_t (which we name l_t^*) is given by a line with a slope ρ^*/tZ which crosses the point $R_T(0)$ as seen in Fig. 4(b),

$$l_t^* = l_t\rho/\rho^*. \tag{4}$$

The correct contact resisticity ρ_c^*, is then given by

$$\rho_c^* = \rho_c\rho/\rho^*, \tag{5}$$

and one can clearly see that ρ_c^* deviates from the customarily measured ρ_c depending on the ratio ρ/ρ^*.

If we now etch between the contact pads to a depth Δt_1 (see Fig. 4(b)), and repeat the TLM of measurements, we find a new contact resistivity ρ_{c1}^* which includes the contribution from the resistivity ρ^* under the contact. If $t \gg \Delta t_1$, we may assume that the current distribution under the contact is only slightly affected, and may still use the TLM (or the ETLM), resulting in

$$\rho_{c1}^* - \rho_{c0}^* = \rho^*\Delta t_1, \tag{6}$$

where ρ_{c0} and ρ_{c1} are the customarily determined contact resistivities for $\Delta t = 0$ and $\Delta t = \Delta t_1$, respectively. Using eqn (5) in (6) leads to

$$\rho^* = [\rho(\rho_{c1} - \rho_{c0})/\Delta t_1]^{1/2}. \tag{7}$$

Note that the analysis presented here is valid only if ρ^* is uniform across the depth of the epilayer under the contact, which is incorrect. Nevertheless, if ρ_i^* is regarded as an average resistivity under the contact below the etching level Δt_i, one could approximately determine ρ_i^* by a step etching process

$$\rho_i^* = [\rho(\rho_{ci} - \rho_{ci-1})/\Delta t_i]^{1/2}. \tag{8}$$

Figure 5 summarizes experimental results on samples with carrier concentrations in the range $(5\times10^{16}$–$1\times10^{18})\,\mathrm{cm}^{-3}$. Results had been deduced from graphs as the ones shown in Fig. 6. The drawn lines are the least square fits to the experimental points. The line representing $i = 4$ leads to a lower ρ_c. At this depth (~ 5500 Å) our approximation is not valid anymore and the results are questionable. As noted later, etching of the contacts themselves starts degrading the contacts too, after a prolonged etching time. As one can clearly see, the resistivity of the contacted material is 5–10 times higher than the uncontacted material and it varies very slightly down to a depth of more than 4000 Å which is similar to the thickness of most epi-layers in actual devices. On the other hand, if one assumes that ρ^* extends only in a thickness of Δt_1 from the top, and the resistivity below this level is ρ, one gets

$$\rho^* = (\rho_{c1} - \rho_{c0})/\Delta t_1, \tag{10}$$

which leads to a ρ^* which is even larger than the one determined by eqn (7).

Note that a slight etching of the GeNi clusters occured during the etching of the GaAs material. Independent tests have shown that this etching degraded the ohmic contacts only slightly and the major contribution to the increase in ρ_c was due to the etching between the pads.

In addition, we have utilized the TLM to find contact resistivity in two similar samples, both Ge doped to $4\times10^{17}\,\mathrm{cm}^{-3}$, but with epi-layer thicknesses of 1000 Å and 1 μm. It was assumed that if a thin layer of different conductivity lies under the contact, we will measure a

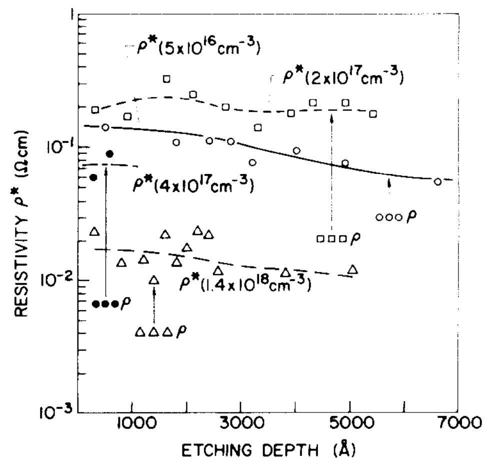

Fig. 5. Experimental results for the resistivity under the contact as a function of depth, for samples with $N_D = (5\times10^{16}$–$1.4\times10^{18})\,\mathrm{cm}^{-3}$. The resistivity of the uncontacted material is shown for reference in each case.

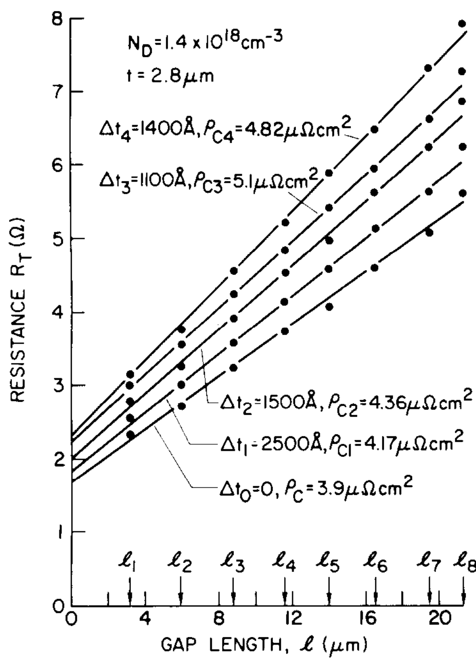

Fig. 6. A demonstration of the method for measuring ρ^* for a sample with $N_D = 1.4 \times 10^{18}\ \mathrm{cm}^{-3}$. Δt_i and ρ_{ci} are the additional etched depth in the grooves and the resultant contact resistivity, respectivly, after etching step i. The lines are the least square fit through the shown experimental points. In the case $i = 4$, the TLM is not applicable any more.

different ρ_c in both cases. For both samples, ρ_c in the range $(5\times10^{-6}$–$1\times10^{-5})\Omega\,\mathrm{cm}^2$ was measured without marked differences between them. This result confirms the hypothesis that if a different conductivity layer exists under the contact, it is probably uniform through the total depth of the epi-layers.

Since the resistance of the underlying layer changes with background carrier concentration (N_D) ρ_c will show a direct dependence on N_D, while ρ_c^* should be constant and much smaller. Let's look at an example where ohmic contacts were formed on an epi-layer with a typical carrier concentration of $2\times10^{17}\ \mathrm{cm}^{-3}$. Assume $\rho_c = 4\times10^{-6}\ \Omega\,\mathrm{cm}^2$ (Fig. 3), $\rho = 0.015\ \Omega\,\mathrm{cm}$ and $\rho^* = 0.2\ \Omega\,\mathrm{cm}$ (Fig. 5). From eqn (6), $\rho_c^* = 3\times10^{-7}\ \Omega\,\mathrm{cm}^2$, and obviously the largest contribution to ρ_c comes from the underlying layer resistivity. If the high resistivity layer results from compensation (due to the Ni diffusion, for example), ρ^*/ρ should decrease with increased N_D, and even if $\rho_c^* = \mathrm{const.}$, ρ_c will show a tendency to decrease with N_D (as was observed for thin eip-layers, and to a lesser extent in thick ones).

5. PERIPHERY EFFECTS

In the process of etching described in IV, we observed that the GaAs along the periphery of the AuGeNi contact is not etched, as shown in Fig. 7(a). This $\sim 1\ \mu\mathrm{m}$ step, which reveals itself only after etching, exists only near the periphery of alloyed GeAuNi contacts, and is not a result of photoresist left-overs or an excessive etching of the GeAuNi above the step (etchant solution was $H_3PO_4:H_2O_2:H_2O$ (3:1:50), with etching rate of $\sim$ 800 Å/min at room temperature). When etching between non-alloyed pads is performed, lateral under-cutting of a few microns is observed under the pads.

In order to identify the cause of that step, 100 Å of Ni was evaporated on the GaAs surface, patterned to squares, and the GaAs was etched to about 1000 Å deep around the Ni pads in samples where the Ni had been heated up to 450° for 30 sec and in samples where it was not heated up. As shown in the picture in Fig. 7(b), the thin Ni was removed in the process of etching and the material under the Ni was etched to a deeper depth than the material outside the contact (by about 200 Å). Between both regions an unetched ridge is clearly seen ($\sim 2\ \mu\mathrm{m}$ wide). Since the material under the heated Ni is being etched faster than the GaAs, incorporation of Ni in GaAs cannot explain the ridge formation. Microprobe analyses were carried on the GeAuNi–GaAs alloyed contact and the Ni–GaAs heated sample in the ridge regions. To the detectibility limit (about 0.1% of GaAs bulk density), no Au, Ge or Ni in the first sample, nor Ni in the second sample were found. No traces of photoresist were found, either. It is likely that stresses under the contact in the process of heating affect structurally the edges which exhibit different etching properties. If these etching-resistant regions have different properties from the uncontacted GaAs layer (especially if their resistance is higher), the effect on the operation of small dimension devices can be critical.

Note that interpretation of results in TLM are now even more ambigious due to the uncertainty of the materials' resistivity near the edges. It is almost certain that this undetermined resistivity is much lower than ρ^*, otherwise l_t would be negative, which has never been observed experimentally (to get l_t positive, $\rho^*/\rho < 1 + l_t/\Delta$, where Δ is the width of the step). In the interpretation of GTLM we have assumed that the resistivity of the step is approximately ρ, otherwise the deduced ρ^* would have a different value.

6. CHARACTERISTICS OF THE ALLOYED AuGeNi SURFACE

Observation of the surface of the contact after alloying reveals distinct dark clusters, as shown in the SEM micrograph of Fig. 8(a). Many of the clusters are elongated with the small dimension of $\sim 0.5\ \mu\mathrm{m}$ and the large dimension of (3–5) μm. By monitoring the x-ray emission resulting from 20 KV electron bombardment (microprobe analysis), these clusters have been identified as GeNi rich and Au deficient, as shown in Fig. 8(b)–(d). Similar results have been reported in Refs. [10, 14, 25–27].

It was observed that contact resistivity is somewhat correlated to the clusters' size and their density. Small and dense clusters produce a lower contact resistivity. These results suggest that the GeNi clusters are responsible for the contact formation, and that the current flows into the semiconductor nonuniformly. Our results contradict the observations of Cristou *et al.*[26, 27], who reported a lower contact resistivity for contacts with larger clusters. Moreover, if one defines the edge of the contact in some contour fashion around the most remote clusters to the edge, edge definition becomes very difficult. In effect, in the TLM of measuring ρ_c, the "real"

distance between the pads should be greater than the distance between the pads' edges. Consequently, the true contact resistivity is smaller than the measured one, and the $\sim 1/N_D$ dependence of ρ_c (which other researchers reported) can be false (this can be easily seen if l_i is replaced by $l_i + \delta$, where δ is the additional effective gap length due to the poor edge definition, and $R_{sh} \propto 1/N_D$, hence ρ_c (measured) $= \rho_c$ (true) $+ (\delta^2 + 2l_t\delta)R_{sh}$ which leads to the $1/N_D$ dependence even when ρ_c (true) is independent of N_D).

7. THE DECOMPOSED LAYER UNDER THE CONTACT

Secondary ion mass spectrometry (SIMS) analysis was conducted on non-alloyed and alloyed samples. In this measurement, primary ions (O_2^+) sputter the surface and the masses of the secondary ions coming off the surface are monitored. The sensitivity of this method is at least an order of magnitude better than Auger or microprobe analyses. Since the sputtering rate of each constituent is different, the surface which is produced is rough, and the depth scale is not the same for all elements. Also, the sputtering ions mix the elements and degrade the resolution. Nevertheless, one gets an estimate of the penetration depth of contact materials and the out diffusion of Ga and As to the surface.

The final distribution of the elements is not affected by the sequence of evaporation, due to their fast diffusion. As was observed before[4, 31, 32] Ga and As move toward the surface and Au, Ge and Ni move into the GaAs. As is seen in Fig. 9(b) (in comparison with Fig. 9(a)), Ga moves toward the surface to a larger extent than As does, probably creating Ga vacancies. Ni and Ge move into the GaAs to a depth of at least 3000 Å, while Au stays closer to the interface. Near the interface, where Ga vacancies exist, Ge can dope the GaAs heavily, but under 1000 Å or so, the abundance of Ni (which is a p-type dopant) and Ga can create a high resistivity layer. (Note, that the peaks of Ga and As near the surface of the non-alloyed sample are most probably false, and result from some resputtering of Ga and As on the surface from the gun, which was coated by them in a previous run.)

8. TEMPERATURE MEASUREMENTS

We have measured the temperature dependence of ρ_c for several samples with doping range $(5 \times 10^{16}$–$2 \times 10^{18})\,cm^{-3}$ between room temperatures and ~ 4°K. Measurements were done by mounting a multipad pattern on a specially designed holder, and dipping it in a dewer where the temperature was varied continuously. The TLM was employed with a four probe configuration, and results are shown in Fig. 10 for one sample. The contact resistance does not change over the temperature range to within the experimental error, which was about ±30%. The lack of temperature dependence is consistent with tunneling through a heavily doped Schottky barrier with a constant barrier height. Models for the contact will be discussed in more detail in the next section.

9. DISCUSSION

The AuGeNi ohmic contact is generally depicted as a Schottky barrier to n^+-type Ge-doped GaAs on top of undisturbed n-type GaAs. This model's band diagram is depicted in Figs. 11(a) and (b). The evidence for the existing n^+-layer under the contact is the tunneling results reported by Holonyak et al.[2, 3], where AuGe (without Ni) contact metallurgy was used. They found that a tunnel diode is obtained when AuGe is alloyed into

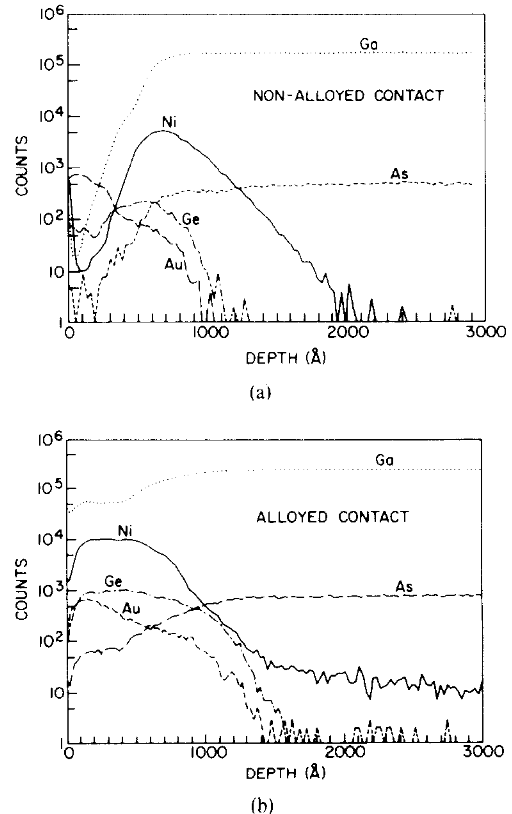

Fig. 9. Results of SIMS measurements of non-alloyed and alloyed GeAuNi on GaAs. (a) Non-alloyed sample (Ga and As peaks on surface are probably an artifact). (b) Alloyed sample. Ni and Ge are diffusing deep into the substrate. Note, that depth scale is not exactly the same for all elements.

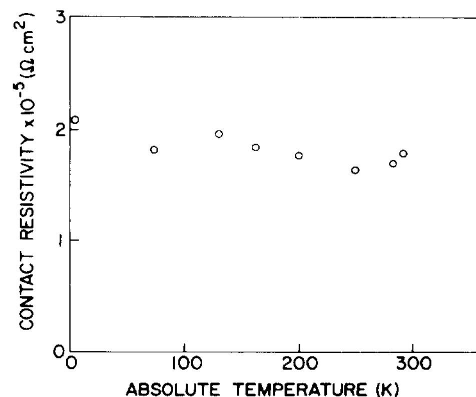

Fig. 10. Temperature dependence of contact resistivity in a sample, Ge doped to $\sim 2 \times 10^{16}\,cm^{-3}$. ρ_c is basically temperature independent.

p^+-GaAs, which requires the formation of the n^+-region. Even though the thickness of the n^+-layer is unknown, Popovič[46] assumed (inexplicitly) that it is very narrow and ballistic transport of the tunneling hot electrons is possible through the n^+-region. Current results only from those electrons in the metal with energies which exceed the n^+–n interface potential barrier, see Fig. 11(b). Since this potential barrier height depends on the n-type doping, Popovič derives an $1/N_D$ dependence for ρ_c. A drop in ρ_c as N_D was increased has been observed by many researchers[13, 40–45], and to a much lesser extent by us, but explaining this phenomenon by exploiting ballistic transport is not proven. On the other hand, if the n^+-layer is thick enough to allow electrons to thermalize after tunneling, one would expect an opposite dependence[57]. It can be easily understood if one takes into account the spill-over of electrons from the n^+-layer into the n-layer. The change in resistance due to this spill-over will be greater for low doped epi-layer, resulting in a lower contact resistance (where is defined as the difference between the total resistance of the sample before and after contacts are formed). Hence, the dependence of ρ_c on N_D should be monotonically positive, which was never observed.

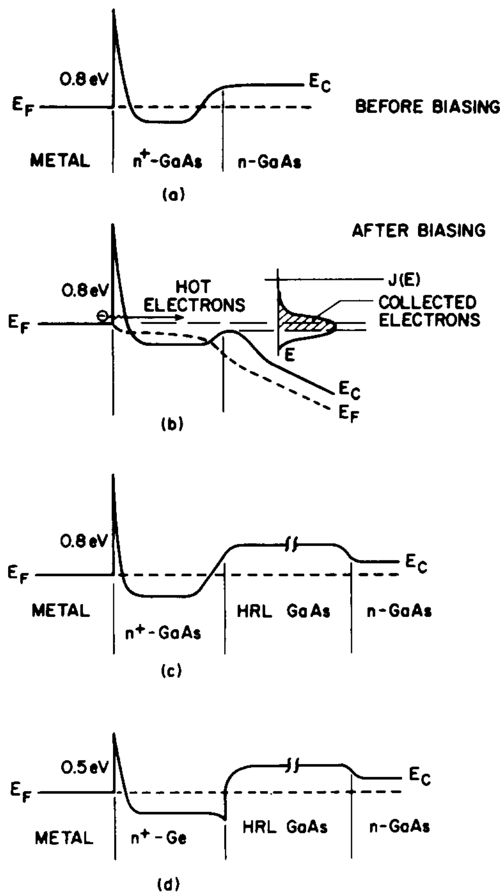

Fig. 11. Models for the AuGeNi ohmic contact. (a) The customarily accepted model. A Schottky-barrier on an n^+-GaAs, Ge-doped, and a transition into the unaffected n-type layer. (b) The same after biasing. (c) A possible model with a high resistivity layer under the contact. Schottky barrier is formed with the GaAs. (d) Another possible model with a high resistivity layer under the contact. Conduction mainly occurs through Ge–Ni rich clusters which are heavily doped by As. Schottky barrier is formed with Ge.

Let's discuss some other possibilities in light of our results. We have observed: (1) a weak dependence of ρ_c on N_D, when relatively thick epi-layers are used in the measurements (Fig. 3); (2) a higher resistance layer (HRL) of an undetermined thickness which contributes to the contact resistance more than the intrinsic contact itself; (3) a zone at the periphery of the contact with different etching properties, and possibly different electrical properties; (4) the dependence of ρ_c on the density (and total area) of the Ge–Ni rich clusters, suggests that conduction occurs mostly through these clusters and makes the real edge of the contact ambiguous; (5) a very weak (if at all) temperature dependence of ρ_c (Fig. 10), suggests tunneling transport through the contact-GaAs interface; (6) a very deep penetration of Ni and Ge into GaAs after alloying (Fig. 9).

The origin of the HRL is unclear, but its existence is not surprising either. There is evidence that the contacted material is not stoichiometric, nonuniform and stressed, and layer decomposition and pits extend all the way from 0.1 to 1.4 μm[11, 14, 15, 29]. These effects can cause the observed HRL. In addition, Magee *et al.*[58] have reported that chromium outdiffuses to the GaAs surface during heat treatment, and layers underlying the ohmic contacts that are extremely rich in chromium have been found[59]. Also, Ni and Au are known p-type dopants in GaAs[34, 49, 50–53]. For example, Ni was found to replace Ga and produce deep acceptor levels, 0.22 eV[49], and 0.35 and 0.44 eV[50] above the valence band. Combined with the Ni high diffusivity (Fig. 9(b) and Refs. [8, 14, 25–30]), a very deep HRL can be produced. Also, an excess Ga (relative to As) moves out from the GaAs leaving an As rich zone under the contact which can lead to a HRL. If one takes into account the HRL, eqn (5), which probably extends throughout most contacted thin epi-layers, the "true" contact resistivity (ρ_c^*) can be an order of magnitude lower than the "measured" one (ρ_c). However, the measured ρ_c is the useful contact resistivity, as long as the HRL cannot be avoided. For thick layers (in excess of 1.5 μm), the contacted material makes a transition from high to normal resistivity along the depth dimension, a fact that complicates the estimate of contact resistivity considerably. In our samples, where thick epi-layers have been used (> 2 μm), the measured contact resistivity shows only a very slight dependence on N_D, possibly because the HRL is only a fraction of the total thickness of the eip-layer. Note that the elimination of Ni from the contact (assuming it is a main contributor to the HRL) does not improve ρ_c, since Ni plays an important role in the diffusion of Ge into GaAs (Section 1 and Fig. 9(b)).

The peripheral zone which we have found around the contact complicates matters even further. This unetched zone is most probably induced by stress, and its electrical characteristics are unknown. Since it extends outward for about 1 μm from the contact edge it modifies (in an unclear way) the characteristics of very small

structures, and certainly the interpretation of the TLM. (Other periphery effects have been found in Al/Si contact[54].)

In light of these results, and the evidence that current is flowing mostly through the Ge–Ni clusters, one could propose different models for the conduction in AuGeNi ohmic contacts, and two are depicted in Figs. 11(c) and (d). Possible tunneling contacts are Au–Ge (Note that the barrier height was found to be 0.3 eV in [5]) or Au–GaAs. The possible n^+-layers are GaAs–Ge doped (with maximum doping in the low 10^{18} cm^{-3} range), or Ge–As doped (which can be as high as 1.4×10^{20} cm^{-3}[54]). The HRL is a modified GaAs layer in both cases.

Since the TLM is very sensitive to the spacing dimensions and the uniformity of the contacted epi layer, a more suitable method has to be adopted for finding ρ_c for AuGeNi contacts, and vertical transport measurements (VTM) are preferable. The one done by Gol'dberg *et al.*[56] is ideal but very combersome, and the standard VTM[39] is not accurate for both: contacts on epi-layers grown on conductive substrates or on bulk materials, since the material resistance cannot be subtracted out accurately. Presently, this leaves us only with a determination of ρ_c from the particular device performance.

10. CONCLUSIONS

We have reviewed extensively the literature and found little theoretical justification for a $1/N_D$ dependence of the contact resistivity. This finding could result from the method of measurement and from a high resistivity layer under the contact, which we have found evidence for. Microprobe and SIMS analyses show that the contact is not uniform at the surface and into the depth. Ge and Ni segregate into Ge–Ni rich clusters on the surface and diffuse deeply into the sample. Ga diffuses heavily into the contact, and As to a lesser extent. Methods of measurements and accepted models are critically reviewed and new possible models are proposed.

Acknowledgements—We wish to thank J. Webber and A. Yen for the SIMS and R. Schad for the microprobe analyses, L. Alexander for helping in the temperature measurements, J. M. E. Harper for ion beam etching, and mostly L. Osterling for his technical help throughout this project.

REFERENCES

1. N. Braslau, J. B. Gunn and J. L. Staples, *Solid-St. Electron.* **10**, 381 (1967).
2. N. Holonyak, Jr., D. L. Keune, R. D. Burnham and C. B. Duke, *Phys. Rev. Lett.* **24**, 589 (1970).
3. A. M. Andrews and N. Holonyak, Jr., *Solid-St. Electron.* **15**, 601 (1972).
4. G. Y. Robinson, *Solid-St. Electron.* **18**, 331 (1975).
5. H. Paria and Hartnagel, *Appl. Phys.* **10**, 97 (1976).
6. J. B. Gunn, *IBM J. Res. Dev.* **10**, 300 (1966).
7. T. E. Hasty, R. Stratton and E. L. Jones, *J. Appl. Phys. Phys.* **39**, 4623 (1968).
8. M. Wittmer, R. Pretorius, J. W. Mayer and M. A. Nicolet, *Solid-St. Electron.* **20**, 433 (1977).
9. H. W. Thim and S. Knight, *Appl. Phys. Lett.* **11**, 83 (1967).
10. N. Yokoyama, S. Ohkowa and H. Ishikawa, *Jap. J. Appl. Phys.* **14**, 1071 (1975).
11. J. S. Harris, Y. Nannichi and G. L. Pearson, *J. Appl. Phys.* **40**, 4575 (1969).
12. C. R. Paola, *Solid-St. Electron.* **13**, 1189 (1970).
13. T. Inada, S. Kato, T. Hora and N. Toyoda, *J. Appl. Phys.* **50**, 446 (1979).
14. M. Ogawa, *J. Appl. Phys.* **51**, 406 (1980).
15. D. C. Miller, *J. Electrochem. Soc.* **127**, 467 (1980).
16. K. Ohata and M. Ogawa, *Proc. 12th Ann. Reliability Physics Symposium*, p. 278. IEEE, New York (1974).
17. H. Murrmann and D. Widmann, *IEEE Trans. Electron Dev.* **ED-16**, 1022 (1969).
18. G. D'Andrea and H. Murrmann, *IEEE Trans. Electron Dev.* **ED-17**, 484 (1970).
19. P. L. Hower, W. W. Hooper, B. R. Cairns, R. D. Fairman and D. A. Tremere, *Semiconductors and Semimetals* (Edited by R. K. Willardson and A. C. Beer), Vol. 7A, p. 179. Academic Press, New York (1971).
20. V. Ya. Niskov and G. A. Kubetskii, *Sov. Phys. Semicon.* **4**, 1553 (1971).
21. H. H. Berger, *J. Electrochem Soc.* **119**, 509 (1972).
22. H. H. Berger, *Solid-St. Electron.* **15**, 145 (1972).
23. G. K. Reeves, *Solid-St. Electron.* **23**, 487 (1980).
24. J. Gyulai, J. W. Mayer, V. Rodriguez, A. Y. C. Yu and H. J. Gopen, *J. Appl. Phys.* **42**, 3578 (1971).
25. W. T. Anderson, Jr., A. Christou and J. W. Davey, *IEEE J. Sol. St. Circut.* **SC-13**, 430 (1978).
26. A. Christou, Solid-St. Electron **22**, 141 (1979).
27. A. Christou and K. Sleger, *Proc. 6th Biennial Cornell Electrical Engineering Conference*, p. 169 (1977).
28. R. B. Gold, R. A. Powell and J. F. Gibbons, *AIP Conf. Proc. Nr.* 50, *Laser-Solid Interactions and Laser Processing* p. 635 (1978).
29. G. Eckhardt, In *Laser and Electron Beam Processing of Materials* (Edited by C. W. White and P. S. Peercy), p. 467. Academic Press, New York (1980).
30. J. L. Tandon, C. G. Kirkpatrick, B. M. Welch and P. Fleming, *Ibid.* p. 487.
31. G. Y. Robinson, *J. Vac. Sci. Technol.* **13**, 884 (1976).
32. B. L. Weiss and H. L. Hartnagel, *Electron. Lett.* **11**, 263 (1975).
33. T. J. Nagee and J. Peng, *Phys. Stat. Sol.* (a) **32**, 695 (1975).
34. M. Otsubo, H. Kumabe and H. Miki, *Solid-St. Electron.* **20**, 617 (1977).
35. S. G. Bandy, R. Senkaran and D. M. Collins, Annual Report No. 3, Varian Association (1979).
36. M. N. Yoder, *Solid-St. Electron.* **23**, 117 (1980).
37. T. Nakamisi, *Jap. J. Appl. Phys.* **12**, 1818 (1973).
38. H. M. Macksey, In *Inst. Phys. Conf. Ser.* *33b* (Edited by L. Eastman), p. 245 (1976).
39. R. H. Cox and H. Starck Solid-St. Electron. **10**, 1213 (1967).
40. H. Matino and M. Tokunaga, *J. Electrochem. Soc.* **116**, 709 (1969).
41. W. D. Edwards, W. A. Hartman and A. B. Torrens, *Solid-St. Electron.* **15**, 387 (1972).
42. K. Heime, U. Köhig, E. Kohn and A. Wartmann, *Solid-St. Electron.* **17**, 835 (1974).
43. K. K. Shih and J. M. Blum, *Solid-St. Electron.* **15**, 1177 (1972).
44. B. P. Johnson and C. I. Huang, *J. Electrochem. Soc.* **126**, 474 (1978).
45. F. Vidimari, *Electron. Lett.* **15**, 675 (1979).
46. R. S. Popovic, *Solid-St. Electron.* **21**, 1133 (1978).
47. B. C. Johnson, C. H. Arpin and W. H. Wadlin, *J. Vac. Sci. Technol.* **16**, 145 (1979).
48. L. J. van der Pauw, *Philips Res. Rep.* **13**, 1 (1958).
49. R. W. Haisty and G. R. Cronin, *Proc. 7th International Conf. Phys. Semicond.* (Edited by M. Hulin). Paris (1964).
50. N. I. Suchkova, D. G. Andrianov, E. M. Omel'yanovskii, E. P. Rashevskay and N. N. Solo'ev, *Sov. Phys. Semicond.* **9**, 469 (1975).
51. W. J. Brown, Jr. and J. S. Blakemore, *J. Appl. Phys.* **43**, 2242 (1972).
52. H. Ennen, U. Kaufman and J. Schneider, *Solid-St. Commun.* **34**, 603 (1980).
53. H. Ennen, U. Kaufman and J. Schneider, *Appl. Phys. Lett.* **38**, 355 (1981).

54. R. K. Tsui and M. Gershenzon, *Appl. Phys. Lett.* **37**, 218 (1980).
55. R. Stall, C. E. C. Wood, K. Board and L. F. Eastman, *Electron. Lett.* **15**, 800 (1979).
56. Yu. A. Gol'dberg and B. V. Tsarenkov, *Sov. Phys. Semicond.* **3**, 1447 (1970).
57. J. J. Rosenberg, E. J. Yoffa and M. I. Nathan, *IEEE Trans. Elect. Dev.*, to be published (1981).
58. T. J. Magee, J. Peng, J. D. Hong, V. R. Deline and C. A. Evans, Jr., *Appl. Phys. Lett.* **35**, 815 (1979).
59. T. J. Magee, Private communication.